AIAA JOURNAL
Vol. 30, No. 11, November 1992

Generalized Vortex Lattice Method for Oscillating Lifting Surfaces in Subsonic Flow

Paulo A. O. Soviero*
Instituto Tecnológico de Aeronáutica, 12225 São José dos Campos, São Paulo, Brazil
and
Marcos Vinícius Bortolus†
Universidade Federal de Minas Gerais, 31270 Belo Horizonte, Minas Gerais, Brazil

A numerical method for calculating the unsteady pressure distribution on harmonically oscillating lifting surfaces in subsonic flow is presented. The Helmholtz equation for the complex velocity potential is written in integral form and solved by discrete panels superposition, which can be recognized as a generalization of the well-known vortex lattice method. Numerical calculations are carried out for a rectangular wing and are compared with well-established literature data. The influence of chordwise and spanwise discretization, as well as wake length, on the convergence rate, is also numerically studied. Good results have been obtained using the present method even for high values of reduced frequency and Mach number.

Introduction

In 1940 Küssner[1] derived the governing integral equation for the problem of the lifting surface oscillating harmonically in a subsonic compressible flow. Today this problem can then be considered a classical one. The reader is referred to Yates[2] for a historical review and a discussion of the state of the art of unsteady aerodynamics.

It is usual in aeroelasticity to use the acceleration potential as the main variable because this quantity is directly proportional to the pressure perturbation. This permits attention to be focused only over the wing because, when crossing this surface, the pressure shows a jump discontinuity. Hence, all of the wake downwash effects are incorporated into the kernel of the integral equation. In this case there are generally two ways of handling the problem. The first method, called "global pressure mode" or "subsonic kernel function," is discussed by Rowe.[3] The second method is represented by the doublet lattice[4] method or by its variant, the doublet point[5] method. The latter approach offers the distinct advantage of not requiring the user to devise suitable pressure-mode functions with appropriate edge conditions and continuities. This important aspect explains its wide acceptability.

Although less widespread than the acceleration potential to treat unsteady compressible aerodynamics, the velocity potential formulation[6,7] is more appealing to the aerodynamicist, whose interests are mostly directed to steady-state problems. The reason for this is the existence of well-known singular solutions as sources, doublets and line vortices, which can be used in subsonic flow and, further, can be retrieved as limiting cases of zero reduced frequency or zero Mach number.

The present paper considers the velocity potential formulation of subsonic flow harmonically oscillating lifting surface problem. The overall treatment is linearized and limited to small disturbances and flat wakes. The solution method is numerical. Wing and wake are both discretized by means of constant density doublet panels, and values of the complex velocity potential are obtained through the solution of the Helmholtz equation. It is shown that these solutions are valid for simultaneously large values of reduced frequency and subsonic Mach number. Convergence studies performed show that in the unsteady flow the wake length necessary to obtain converged solutions is smaller than that in the steady-state case. Moreover, attention is also paid to the fact that the well-known incompressible equivalence between closed vortex loops and surfaces of constant density potential must be complemented in the compressible regime by a surface integral proportional to the square of a parameter K that combines the reduced frequency and the subsonic Mach number.

Received Aug. 19, 1991; revision received Feb. 13, 1992; accepted for publication Feb. 24, 1992.

*Professor, Aeronautical Engineering Division.
†Assistant Professor, Mechanical Engineering Department.

Mathematical Flow Model

In a reference frame that translates steadily, the nondimensional perturbation velocity potential ζ due to small-amplitude motion of a flat wing and wake is governed by the linear convected wave equation,

$$\nabla^2\zeta - \frac{1}{a_\infty^2}\left[\frac{\partial}{\partial t} + V\frac{\partial}{\partial x}\right]^2\zeta = 0 \tag{1}$$

where the undisturbed velocity V is in the positive x direction and a_∞ is the undisturbed speed of sound.

For a harmonically oscillating body in a steady flow, the perturbation velocity potential may be written as

$$\zeta(x, y, z, t) = \exp(i\omega t)\,\hat{\phi}(x, y, z) \tag{2}$$

where ω is the angular frequency of oscillation.

Introducing relation (2) into Eq. (1), transforms Eq. (1) to

$$\beta^2\hat{\phi}_{xx} + \hat{\phi}_{yy} + \hat{\phi}_{zz} - (2i\omega V/a_\infty^2)\hat{\phi}_x + (\omega^2/a_\infty^2)\hat{\phi} = 0 \tag{3}$$

where $\beta^2 = (1 - M^2)$ and M is the undisturbed flow Mach number.

Defining a new complex potential,

$$\phi = \exp[-i\omega Vx/(a_\infty\beta)^2]\hat{\phi} \tag{4}$$

and using the Prandtl-Glauert transformation,

$$X = x/L;\ Y = y\beta/L;\ Z = z\beta/L \tag{5}$$

Equation (3) can be rewritten as the Helmholtz equation; i. e.,

$$\nabla^2\phi + K^2\phi = 0 \tag{6}$$

where

$$K = \omega L/(a_\infty \beta^2) \tag{7}$$

and L is a reference length.

When K is compared with the reduced frequency,

$$kr = \omega L/V \tag{8}$$

it is readily shown that

$$K = krM/(1 - M^2) \tag{9}$$

The reader can observe the dependence of K on Mach number and reduced frequency in Fig. 1. It can be seen that, for high reduced frequencies, the compressibility effect, as a result of high K, may be neglected if the flow Mach number is sufficiently small. The converse statement is also true.

The preceding verification is a very important aspect related to kernel functions simplifications which lead to the classical panel method formulation.[7] From this point of view, compressibility effects are important only for high reduced frequencies and high Mach numbers. Certainly, the boundaries between incompressible and compressible linearized flows are not well defined, and only comparison between both formulations (i.e., $K = 0$ and $K \simeq 0$) can furnish an insight into the relative importance of compressibility.

To complete the mathematical model description, the Helmholtz equation boundary conditions for the problem at hand are as follows: The complex pressure coefficient for unitary values of the undisturbed velocity and reference length is

$$C_p = -2\exp(iKMX) \cdot \left[\frac{iK}{M}\phi + \frac{\partial \phi}{\partial X}\right] \tag{10}$$

When applied to both sides of the wake pressure, continuity is ensured if

$$\delta C_p = 0 = \frac{iK}{M}\delta\phi + \frac{\partial \delta\phi}{\partial X} \tag{11}$$

where $\delta\phi$ and δC_p indicate, respectively, velocity potential and pressure coefficient differences between wake lower and upper sides.

The condition of zero relative normal velocity on the wing becomes, in the transformed plane,

$$\frac{\partial \phi}{\partial Z} = \frac{\exp(-iKMX)}{\beta}\left[\frac{\partial h}{\partial X} + ikrh\right] \tag{12}$$

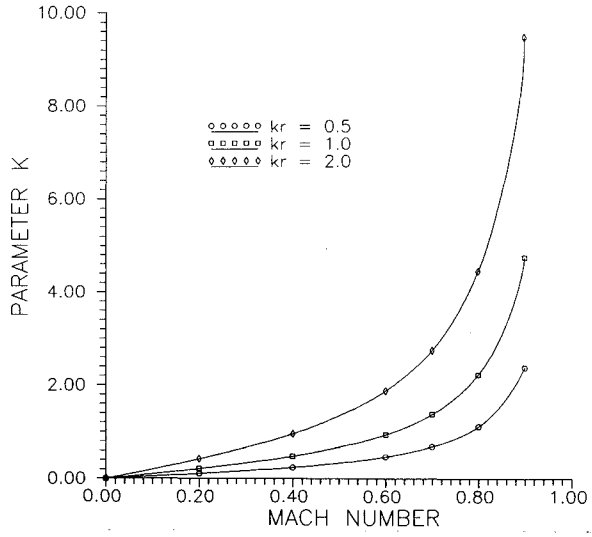

Fig. 1 Mach number and reduced-frequency effects on K.

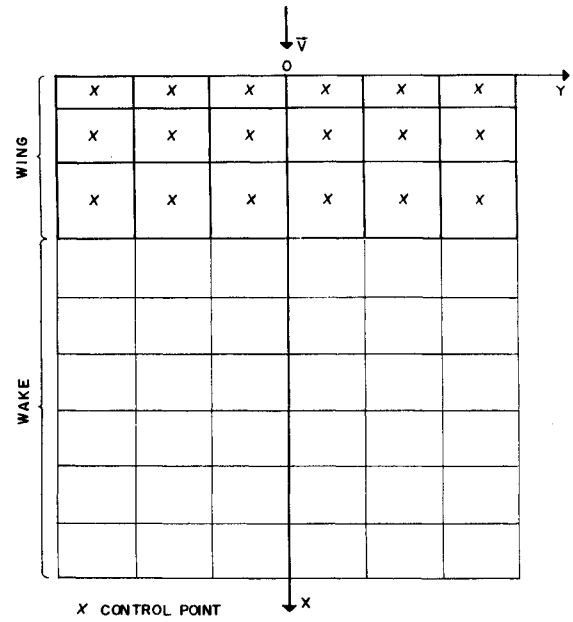

Fig. 2 Overall wing and wake discretizations.

where $h(X, Y)$ is the lifting surface nondimensional vertical displacement amplitude.

Integral Equation and its Numerical Solution

Solution of the problem is obtained by solving Eq. (6), subjected to boundary conditions (11) and (12), for the wake and the wing, respectively.

The integral equation that relates the velocity potential jump across the lifting surface and wake to the velocity potential in the field, can be expressed as[8]

$$\phi_P = \frac{1}{4\Pi}\iint \delta\phi \frac{\partial}{\partial n}\left[\frac{\exp(-iKR)}{R}\right] dS \tag{13}$$

where ϕ_P is the velocity potential in an arbitrary field point $P(X, Y, Z)$, R is the distance from a surface point to P, and n is the unit vector normal to the wing.

The velocity component normal to the wing surface is obtained by taking the Z partial derivative of Eq. (13) and reads

$$\frac{\partial \phi_P}{\partial Z} = \frac{1}{4\Pi}\iint \delta\phi \frac{\partial^2}{\partial Z \partial n}\left[\frac{\exp(-iKR)}{R}\right] dS \tag{14}$$

This equation allows a physical interpretation along the same lines of thought as in the incompressible case. In fact, it can be stated that the integrand represents a normal doublet density $\delta\phi$, distributed over an area element dS. If, in the discretization procedure, $\delta\phi$ is made constant over each element, the well-known vortex lattice method for incompressible flow is recovered, simply by making $K = 0$.

As a numerical application, a rectangular wing divided in $NX \times 2NY$ panels, where NX and $2NY$ refer to chordwise and spanwise directions, respectively, is solved. The wake is modeled by a mesh using NC chords long in the streamwise direction.

Over each panel the doublet density is taken as constant. The boundary conditions are enforced at control points defined at the panels' geometrical centers. The overall discretization grid is shown in Fig. 2.

The numerical scheme that results from discretization of Eqs. (11), (12), and (14) corresponds to a system of linear complex equations written as

$$[a_{k,j}] \cdot [\delta\phi_k] = [F_k] \tag{15}$$

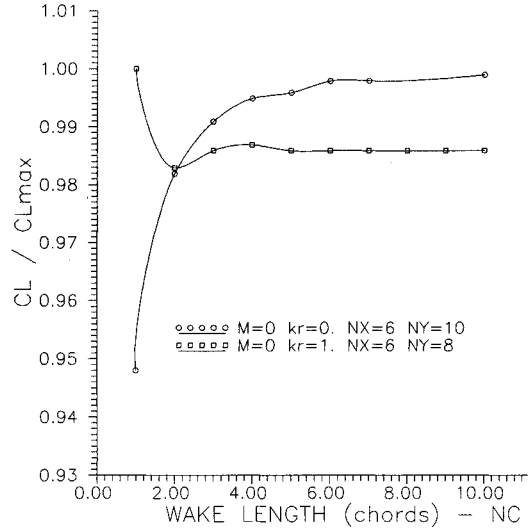

Fig. 3 Wake length influence on lift coefficient amplitude.

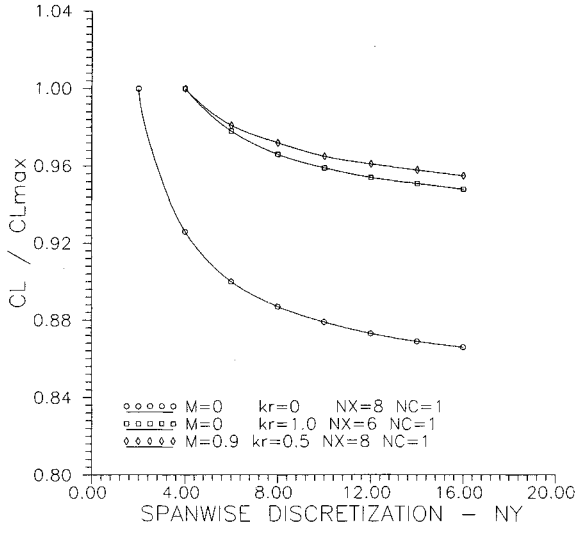

Fig. 4 Spanwise discretization influence on lift coefficient amplitude.

where

$$a_{k,j} = c_{k,j} + b_{k,j} \tag{16}$$

are the complex influence coefficients; $c_{k,j}$ is the normal velocity induced by a wing panel j at another wing panel control point k for $\delta\phi_j = 1$. For wing panels that are in contact with the wing trailing edge,

$$b_{k,j} = \sum_{w=1}^{NXE} \left\{ \exp\left[\frac{iK}{M} (X_j - X_w) \right] c_{k,w} \right\} \tag{17}$$

and for all of the other wing panels, $b_{k,j} = 0$. Equation (17) takes into account continuity of pressure over the wake, as imposed by Eq. (11). In Eq. (17) NXE is the total number of wake panels in the streamwise direction, X_w is the streamwise coordinate of the wake panel center, which has the same Y coordinate of the k wing panel; and $c_{k,w}$ is the induced normal velocity by the w wake panel in the k wing panel control point.

The preceding formulation implicitly satisfies the Kutta condition by imposing equal values of $\delta\phi$ for wing and wake panel rows on each side of the trailing edge. The right-hand side of Eq. (15) is obtained from Eq. (12) calculated at each wing panel control point. In all cases treated in the present formulation, the $a_{k,j}$ values are obtained numerically; nevertheless for $K = 0$ analytical integration may be performed.

To improve convergence, discretization steps in the chordwise direction can be made smaller near the leading edge. Such a discretization will reflect the square root behavior of doublet distribution that is typical of lifting surface theory. However, in the present application all of the wake panels have been equally spaced.

Once the complex system given in Eq. (15) has been solved for $\delta\phi$, the pressure coefficient is determined using Eq. (10) where X derivatives are obtained through the use of classical three-point formulas, with the exception of the leading-edge panels. For these panels it is assumed that

$$\delta\phi(X, Y_0) = AX^{1/2} + BX + CX^2 + D \tag{18}$$

where Y_0 indicates a particular wing section in the spanwise direction. The constants are determined by making $\delta\phi(0, Y_0) = 0$. A better approximation for derivatives near the leading edge is justified, since here local C_p values have a strong influence on global aerodynamic coefficients.

Results and Discussion

The numerical calculations using the present method have been performed for a rectangular wing with aspect ratio two oscillating in pitch around midchord position with a unit pitch angle amplitude. The reference length L was taken as the half-chord at the wing root.

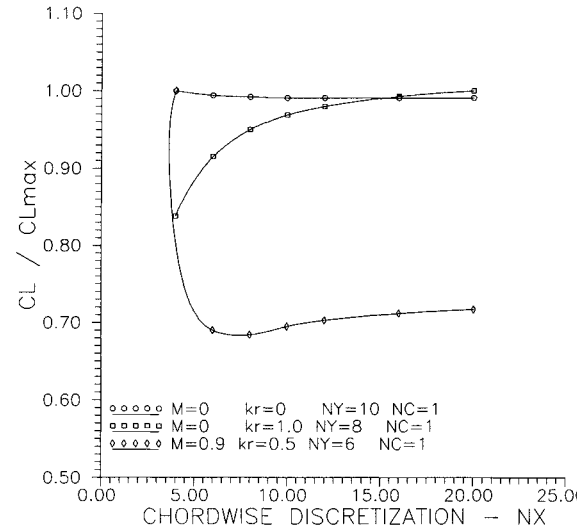

Fig. 5 Chordwise discretization influence on lift coefficient amplitude.

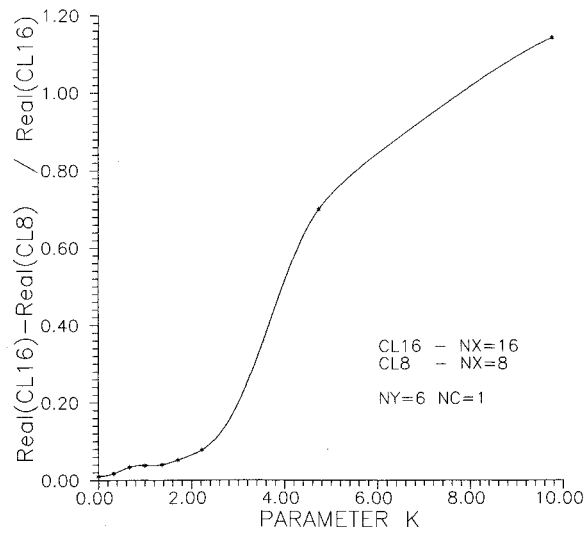

Fig. 6 Influence of K on relative real lift coefficient variation.

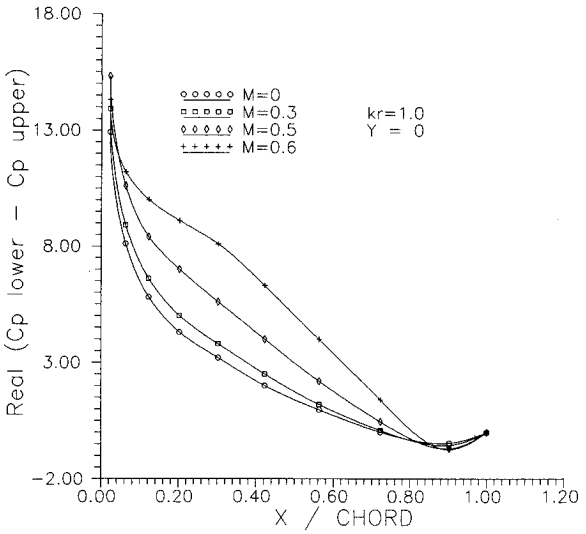

Fig. 7 Real pressure coefficient difference for low subsonic Mach number.

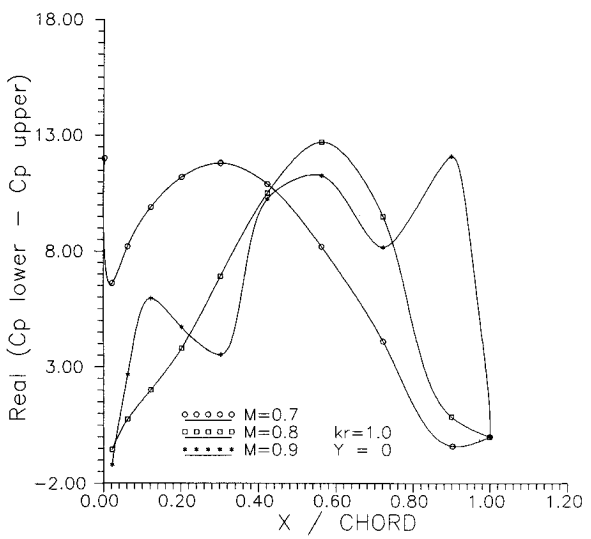

Fig. 8 Real pressure coefficient difference for high subsonic Mach number.

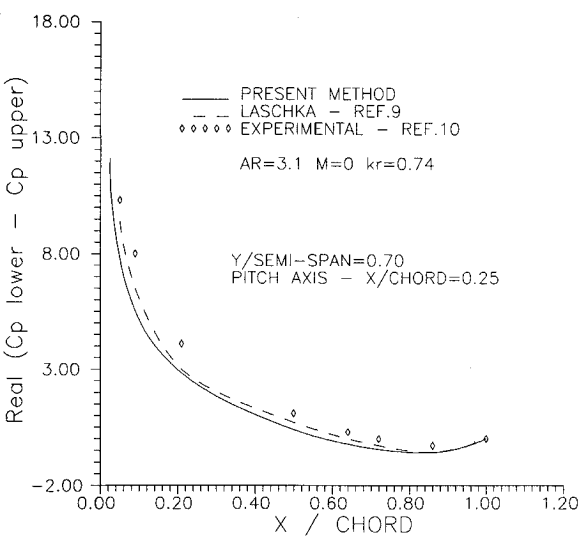

Fig. 9 Real pressure coefficient difference along the wing chord at $Y = 0$.

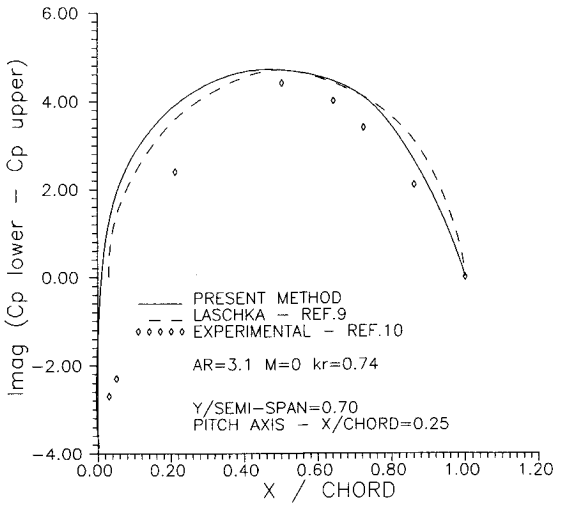

Fig. 10 Imaginary pressure coefficient difference along the wing chord at $Y = 0$.

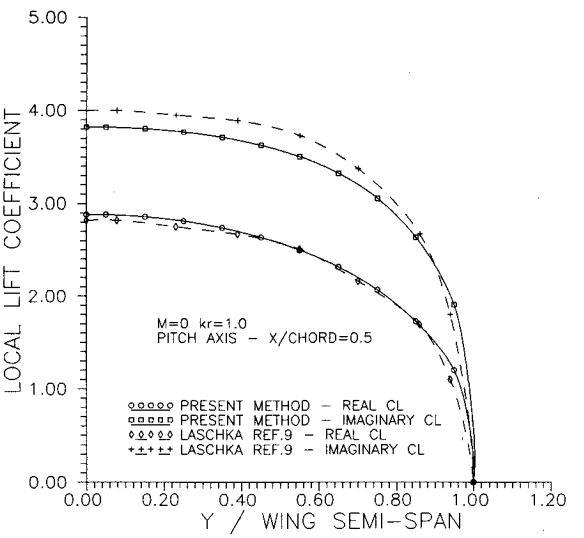

Fig. 11 Local lift coefficient distributions along the wing semispan.

In Fig. 3 the influence of wake length, *NC*, on the convergence of the lift coefficient amplitude calculations is studied. For $NC = 3$, convergence for the steady-state case is practically attained; the lift coefficient amplitude difference is $< 1\%$ compared to the value for $NC = 10$. For unsteady cases, both incompressible and compressible, the same conclusions are obtained with $NC = 2$ and 1, respectively. The wavy behavior of convergence history in the oscillatory incompressible case may be because vortices of different sign are shed alternatively at the trailing edge. This implies a weaker wake length influence compared to that for the steady-state case. The compressible flow case, not shown in Fig. 3, requires a smaller wake length, since K is higher.

The influence of spanwise discretization, *NY*, on the lift coefficient amplitude is shown in Fig. 4. Qualitatively, for all cases presented convergence histories are monotonic and less critical when going from the steady state to the unsteady compressible case. Although convergence is not achieved, extrapolation procedures[3] can be applied in order to enhance prediction accuracy.

Finally, in Fig. 5 the chordwise discretization influence on the lift coefficient amplitude is presented. Here the overall tendency, as observed in Figs. 3 and 4, is reversed; that is, the chordwise discretization for convergence must be increased when going from the steady state to the unsteady compressible

flow. Figure 6 shows the relative variation of the real lift coefficient as a function of K for solutions with $NX = 8$ and 16 and where two regions can be devised. From $K = 0$ to $K = 2$ the percent difference between real lift coefficients is $< 5\%$; for $K > 2$ a sharp divergence occurs that requires a finer discretization for these large values of K. This behavior may be better understood by observing Figs. 7 and 8. Plotted in these figures are values of the real part of the pressure coefficient difference. This is the difference between coefficients on both sides of the wing and referred to its central section. A variation of the Mach number is made at a constant reduced frequency. It can be observed that the pressure coefficient difference maintains its qualitative incompressible behavior until $M = 0.6$; after this, oscillatory distribution becomes predominant, thus requiring finer chordwise discretization.

In the second series of figures presented, the results of the present calculations are compared with other methods available in the literature. Figures 9 and 10 show real and imaginary parts of the pressure coefficient difference for a rectangular wing with an aspect ratio of 3.1. The wing oscillates around a pitch axis through the quarter-point chord in an incompressible flow. The present calculations are compared with those obtained by the kernel-function method of Laschka.[9] Experimental points[10] shown in the figure are only for reference purposes.

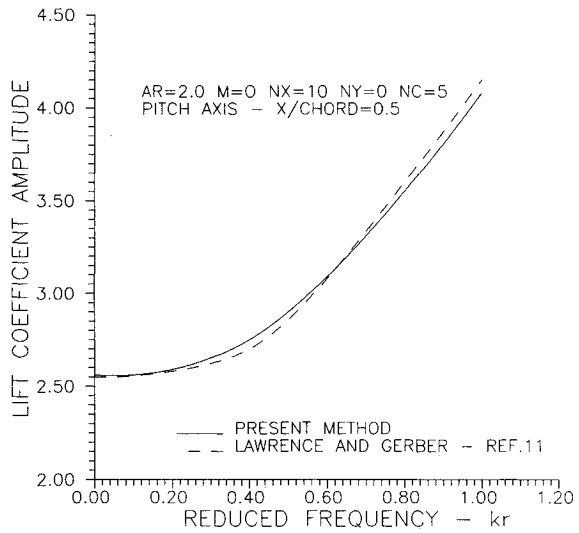

Fig. 12 Reduced-frequency influence on lift coefficient amplitude (incompressible case).

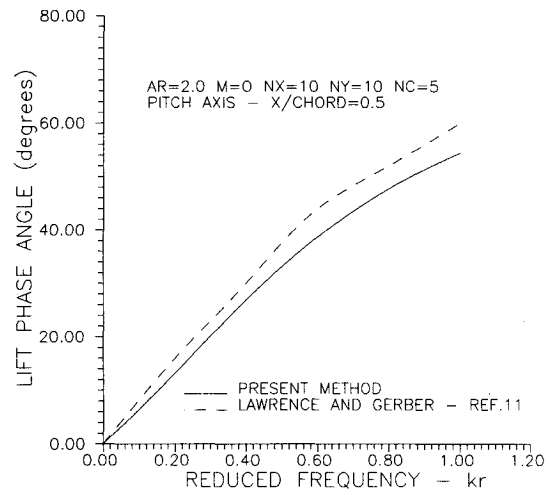

Fig. 13 Reduced-frequency influence on lift phase angle (incompressible case).

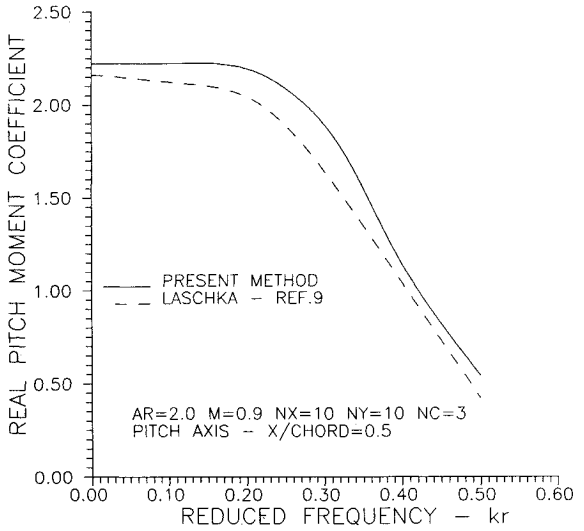

Fig. 14 Reduced-frequency influence on real pitch moment coefficient (compressible case).

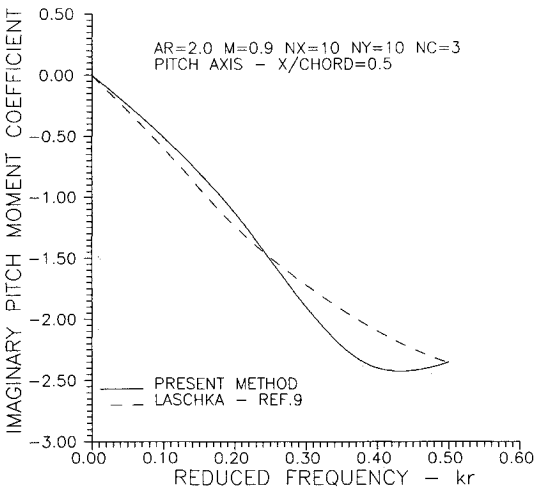

Fig. 15 Reduced-frequency influence on imaginary pitch moment coefficient (compressible case).

In Figure 11 real and imaginary local lift coefficient distributions along the wing span are compared with those of Ref. 9 for a rectangular wing with an aspect ratio of 2. The wing oscillates around a pitch axis through the midchord in an incompressible flow. Despite a small deviation in the imaginary part, overall agreement is quite good. Furthermore, when compared with the doublet point method of Ueda and Dowell,[5] the imaginary distributions are practically coincident.

In Figs. 12 and 13, for the same physical situation as that described earlier (Fig. 11), the lift coefficient amplitude and the phase angle are plotted for several reduced frequencies and compared with the results of Ref. 11. There is a good agreement for the lift coefficient amplitudes, whereas the lift phase angle presents a discrepancy not greater than 10% in the worst case. In the compressible flow case, real and imaginary pitch moment coefficients are compared with calculations from Ref. 9 for several reduced frequencies (see Figs. 14 and 15). However, one can observe an overall agreement concerning the real pitch moment coefficient for larger reduced frequencies, with values of the imaginary part obtained by the model here proposed show an opposite trend.

Finally, the two-dimensional pressure coefficient difference for a pitch oscillation around an axis through the leading edge has been calculated and compared in Fig. 16 with results of

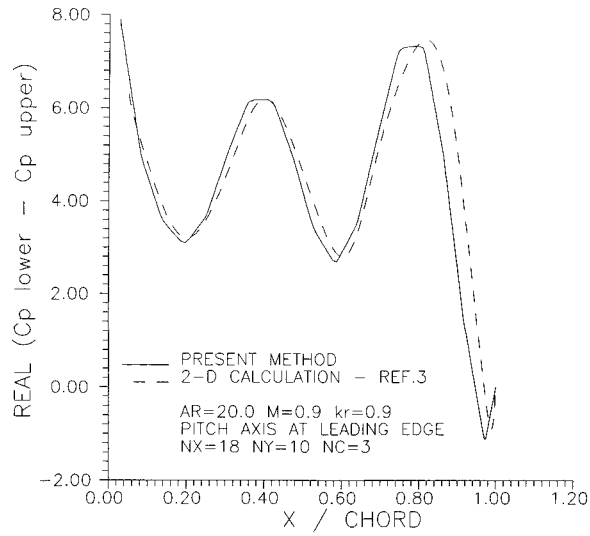

Fig. 16 Two-dimensional real pressure coefficient difference along the profile chord.

Ref. 3. The two-dimensional characteristics are obtained at the central plane of a rectangular wing with an aspect ratio of 20. All of the panels have the same length in the chordwise direction. As can be observed, the general agreement is fairly good for such a high reduced frequency and Mach number combination.

Final Remarks

In the following, the most important characteristics of the model here proposed are emphasized.

The well-known notions of vortex lines and doublets are extended to the compressible range with exactly the same physical meaning that they have in the incompressible formulation. In fact, the incompressible case is a limiting situation that can be recovered from the compressible model by simply making $K = 0$.

The wake is explicitly modeled; Consequently, the kernel functions are simpler.

The general vortex lattice, characterized by constant doublet density, may be easily extended to work with more sophisticated distributions, as for example linear or quadratic doublet densities, without worsening kernel singularities.

Convergence analysis has shown that modeling of the wake has to be accomplished only for few chord lengths. As the values of K increase, this length gets shorter, which is definitely a good feature for high reduced frequencies and Mach numbers.

For more complex geometries, such as nonplanar lifting surfaces, application of the proposed method is straightforward. In fact, even a generalization that takes into account the source term of the integral equation (13) is readily possible (see Ref. 8, p. 498). In this case, thickness effects of wings and fuselages may be accounted for. This extension has already been proposed in Ref. 7 for small values of K.

Appendix: Induced Velocity by a Constant Doublet Panel

The Helmholtz equation admits a singular source solution, which, for an intensity of 4Π units can be written as

$$\phi_s(X, Y, Z) = -\exp(-iKR)/R \tag{A1}$$

where

$$R = [(X - X')^2 + (Y - Y')^2 + (Z - Z')^2]^{1/2} \tag{A2}$$

The singular doublet, whose axis is directed along n, is given by

$$\phi_D(X, Y, Z) = n^* \nabla [-\exp(-iKR)/R] \tag{A3}$$

where ∇ is the gradient operator, and the asterisk indicates a scalar product.

For a panel S, whose normal is also n, a constant-density doublet distribution $\delta\phi$ induces, in a field point $P(X, Y, Z)$, a velocity

$$V_P = \frac{\delta\phi}{4\Pi} \iint \nabla [n^* \nabla \phi_s] \, dS \tag{A4}$$

From the Stokes theorem one can write

$$\int (dl \hat{} \nabla \phi_s) = \iint [(n^* \nabla) \nabla \phi_s + n \hat{} \nabla \hat{} \nabla \phi_s - n^* \nabla^* \nabla \phi_s] \, dS \tag{A5}$$

where l is the panel boundary line and dl is an oriented line differential. The symbol $\hat{}$ indicates a vector product.

Applying the vector identity

$$\nabla(a^*b) = (a^* \nabla)b + (b^* \nabla)a + (a \hat{} \nabla \hat{} b) + (b \hat{} \nabla \hat{} a) \tag{A6}$$

to the integrand of Eq. (A4), we obtain

$$\nabla(n^* \nabla \phi_s) = (n^* \nabla) \nabla \phi_s \tag{A7}$$

since $\nabla \hat{} \nabla \phi_s = 0$, and n is a function of primed variables over S.

Considering Eq. (A7) and the identity

$$\nabla^* \nabla \phi_s = \nabla^2 \phi_s = -K^2 \phi_s \tag{A8}$$

Equation (A5) can be written as

$$\int (dl \hat{} \nabla \phi_s) = \iint [\nabla(n^* \nabla \phi_s) + K^2 n \phi_s] \, dS \tag{A9}$$

When Eqs.(A9) and (A4) are compared, the induced velocity becomes

$$V_P = \frac{\delta\phi}{4\Pi} \left[(dl \hat{} \nabla \phi_s) - K^2 \iint \phi_s n \, dS \right] \tag{A10}$$

This result justifies the generalized vortex lattice concept, since, for $K = 0$, the incompressible case is recovered.

From a numerical standpoint, the influence coefficients elements $a_{k,j}$ may be obtained, for $\delta\phi = 1$, from either Eq. (A4) or Eq. (A10). In the latter case, the line integral over l has an analytic solution. The surface integral, although numerically calculated, is continuous across the panel.

References

[1]Küssner H. G., "General Airfoil Theory," NACA TM 979, 1941.

[2]Yates, E. C., Jr., "Unsteady Subsonic and Supersonic Flows—Historical Review; State of the Art," *Computational Methods in Potential Aerodynamics,* Springer-Verlag, Berlin, 1985, pp. 96–137.

[3]Rowe, W. S., "Comparison of Analysis Methods Used in Lifting Surface Theory," *Computational Methods in Potential Aerodynamics,* Springer-Verlag, Berlin, 1985, pp. 198–239.

[4]Albano, E., and Rodden, W. P., "A Doublet—Lattice Method for Calculating Lifting Distributions on Oscillating Surfaces in Subsonic Flows," *AIAA Journal,* Vol. 7, No. 2, 1969, pp. 279–285.

[5]Ueda, T., and Dowell, E. H., "A New Solution Method for Lifting Surfaces in Subsonic Flow," *AIAA Journal,* Vol. 20, No. 3, 1982,

pp. 348–355.

[6]Haviland, J. K., and Yoo, Y. S., "Downwash-Velocity Potential Method for Oscillating Surfaces," *AIAA Journal,* Vol. 11, No. 5, 1973, pp. 607–612.

[7]Morino, L., and Kuo, C.-C., "Subsonic Potential Aerodynamics for Complex Configurations: A General Theory," *AIAA Journal,* Vol. 12, No. 2, 1974, pp. 191–197.

[8]Lamb, Sir H., *Hydrodynamic* (6th ed.), Cambridge Univ. Press, Cambridge, England, UK, 1975, pp. 498–503.

[9]Laschka, B., "Zur Theorie der Harmonischen Schwingenden Tragenden Fläche bei Unterschallanströmung," *Zeitschrift für Flugwissenschaften,* Vol. 11, No. 7, 1963, pp. 265–292.

[10]Treibstein, H., and Wagener, J., "Druckverteilungsmessungen an einem Harmonischen Schwingenden Pfeilflugel mit zwei Rudern in Incompressible Strömung," DFVLR-AVA-Bereicht 70 J04, Göttingen, Germany, 1970.

[11]Lawrence, H. R., and Gerber, E. H., "The Aerodynamic Forces on Low Aspect Ratio Wings Oscilalating in an Incompressible Flow," *Journal of the Aeronautical Sciences,* Vol. 19, No. 11, 1952, pp. 769–781.